

pubs.acs.org/Macromolecules Article

Effect of Block Number and Weight Fraction on the Structure and Properties of Poly(butylene terephthalate)-block-Poly(tetramethylene oxide) Multiblock Copolymers

Hui Xie,[†] Huanjun Lu,[†] Zhilan Zhang, Xiaohong Li, Xiaoming Yang, and Yingfeng Tu*



Cite This: *Macromolecules* 2021, 54, 2703–2710



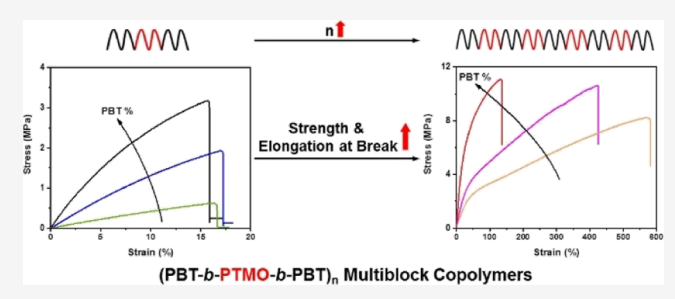
ACCESS

III Metrics & More

Article Recommendations

s Supporting Information

ABSTRACT: We report here the influence of block number and polyester weight fraction on the properties of a series of poly(ether ester) multiblock copolymers (mBCPs), poly(butylene terephthalate)-block-poly(tetramethylene oxide) (PBT-b-PTMO-b-PBT)_n, with the same PTMO segment length. These mBCPs are double-crystalline polymers, where the melting temperature and crystallinity of PBT increase with the polyester weight fraction. The PBT and PTMO blocks undergo phase separation at room temperature to form a plausible bicontinuous disordered structure. With the increment of the block number, the phase-separation-



domain size decreased. As a result, the crystallinity of PBT and PTMO decreases, while the strength and elongation at break of mBCPs increase significantly due to the enhancement of bridging segments between different domains. The increment of the polyester weight fraction significantly enhances mBCPs' strength and Young's modulus but decreases their elongation at break. Our results enrich the understanding on the phase behavior of mBCPs, and the structure—property relationship revealed here would be useful for the design of poly(ether ester) elastomers with desired properties.

INTRODUCTION

Block copolymers can undergo microphase separation to form a variety of ordered structures due to the thermodynamic incompatibility between block components. ^{1–5} Until now, the self-assembled phase-separation behavior of linear AB diblock copolymers is well understood, as they are the simplest system in block copolymers. ^{6–8} However, understanding the phase-separation behavior of multiblock copolymers (mBCPs) is still at a primitive stage, due to the plenty of variables in mBCPs' molecular architecture. ^{9–14} These include the primary factors such as the polymer topology, block numbers, number of block types, degree of polymerization of each blocks, and the Flory—Huggins interaction parameters between different segments, as well as the secondary factors such as polydispersity and subblock structures. ¹⁵ These varieties expand the possible structures of mBCPs to an endless scope and lead to abundant phase behaviors.

Although theoretically mBCPs with any architecture can be obtained via modern synthetic tools such as sequential living/controlled polymerizations, ^{16–23} their synthesis is still difficult and time-consuming. Thus, obtaining different types of mBCPs for just the aesthetic purpose is not practical. Investigations on mBCPs should enhance the understanding on how architectures affect their phase-separation structures as well as properties, to guide the polymer scientists to design mBCP architectures for desirable applications. Since the hard domains can serve as thermally reversible cross-links while the soft

domains as the elastic energy-absorbing region, mBCPs are widely used as thermoplastic elastomers, including different types of polyolefins, polyurethanes, and poly(ether ester)-s.^{23–28} Among them, the mechanical properties are the most important properties for their applications. Bates' group reported a series of elegant works on the polyolefin-based mBCPs' architecture on their phase-separation structures and correlated these to mechanical properties.^{29–34} They found that the microphase structure is affected by mBCPs' primary architecture factors, in addition to the annealing history and others.^{32–34} However, until now, only a few works have reported how the architecture affects mBCPs' mechanical properties,^{35–39} probably due to the synthetic difficulties in obtaining a series of mBCPs with only one architecture factor different.

On the other hand, step-growth polymerization is also an efficient way for the synthesis of mBCPs due to its facile process and economical benefits.^{39–45} The commercially available products include polyurethanes and poly(ether ester)s. For example, Hytrel is a commercialized poly(ether

Received: December 18, 2020 Revised: February 15, 2021 Published: March 2, 2021





$$H = \left\{ \begin{array}{c} \begin{array}{c} \begin{array}{c} \\ \\ \end{array} \\ \end{array} \right\} \left[\begin{array}{c} \\ \\ \end{array} \right] \left[\begin{array}{c} \\ \end{array} \right] \left[\begin{array}{c} \\ \\ \end{array} \right] \left[\begin{array}{c} \\$$

(PBT-b-PTMO-b-PBT)_n Multiblock Copolymers

P1: Feeding ratio (w/w) of PTMO/COBTs = 1:1 P2: Feeding ratio (w/w) of PTMO/COBTs = 2:1 P3: Feeding ratio (w/w) of PTMO/COBTs = 3:1

Figure 1. Structure of the studied (PBT-b-PTMO-b-PBT), mBCPs.

Table 1. Summary of the Chemical Structure of (PBT-b-PTMO-b-PBT)_n mBCPs

sample	feeding ratio ^a	$N_{ m BT}^{b}$	$N_{\rm TMO}^{b}$	$M_{\rm n}^{b}$ (kg/mol)	$w_{\rm PTMO}^{b}$	n^c	block number ^d	$[\eta]$ (dL/g)
P1-1	1/1	16.0	54.6	7.0	50	1.2	3.4	0.47
P1-2		65.5	195	25.2	50	4.3	9.6	1.05
P2-1	2/1	19.2	151	13.8	68	3.2	7.4	0.63
P2-2		56.1	383	35.5	67	8.1	17.2	1.19
P3-1	3/1	13.2	174	14.0	77	3.6	8.2	0.61
P3-2		46.2	568	45.5	77	11.8	24.6	1.14

"Feeding weight ratio of PTMO to COBTs. b Total repeat units of BT ($N_{\rm BT}$) and TMO ($N_{\rm TMO}$), number-average molecular weight of mBCPs ($M_{\rm n}$), and weight content of PTMO ($w_{\rm PTMO}$) in mBCPs, as estimated from NMR spectroscopy. Average repeating units of PBT-b-PTMO-b-PBT segments in (PBT-b-PTMO-b-PBT), mBCPs. Average block number equals to (2n + 1).

ester) elastomer developed by DuPont, 46 using poly-(tetramethylene oxide) (PTMO) as a soft segment and poly(butylene terephthalate) (PBT) as a hard segment synthesized by typical condensation polymerizations. The drawback is the poor control over mBCP's architecture, which is hard for the investigation on the structure—property relationship.

Recently, we have developed a cascade polycondensationcoupling ring-opening polymerization (PROP) method for the facile synthesis of poly(ether ester) mBCPs, utilizing polyether diols as an initiator and cyclic oligoesters as a monomer. 47-Due to the cascade coupling of two polymerizations, poly(ether ester) mBCPs with high molecular weights can be obtained quickly (about 1 h). The side reactions in traditional condensation polymerization are deeply suppressed in PROP by reducing the polymerization time, and mBCPs with a better controlled structure are obtained. We have previously reported the synthesis of (PBT-b-PTMO-b-PBT), mBCPs via PROP, but how the primary architecture factors affect their properties is not clear. In this work, we would like to study the phaseseparation structure and properties of a series of mBCPs with different block numbers and weight fractions. The PTMO segment length is kept constant (molecular weight 2900) to simplify our studies. Our results show that the increment of the block number significantly increases the elongation and tensile strength of the mBCPs but reduces the phase-separationdomain size, while the polyester weight fraction increases the Young's modulus of the elastomers.

■ EXPERIMENTAL SECTION

Materials. Dihydroxyl-terminated PTMO with number-average molecular weights of 2900 g/mol was purchased from Sigma-Aldrich. Cyclic oligo(butylene terephthalate)s (COBTs) were purchased from Star-Better (Beijing) Chemical Materials Co. Ltd. Titanium tetrabutoxide $(\text{Ti}(n\text{-}\text{C}_4\text{H}_9\text{O})_4)$ (Alfa Aesar, 98%) and all other chemicals were used as received.

Synthesis of (PBT-*b***-PTMO**-*b***-PBT)**_n **mBCPs.** The mBCPs were synthesized via cascade PROP using the PTMO diol as an initiator and COBTs as a monomer, according to our previous report provided

in the Supporting Information (Scheme S1 and Table S1).⁴⁸ The products were coded as P1, P2, and P3 samples with a PTMO to COBT feeding weight ratio of 1:1, 2:1, and 3:1, respectively, with the block number controlled by the polymerization time and temperature.

■ RESULTS AND DISCUSSION

Figure 1 shows the chemical structure of obtained (PBT-*b*-PTMO-*b*-PBT)_n mBCPs. To study the architecture effect on properties, three series of mBCPs with different block weight contents were synthesized, with the PTMO to COBT feeding ratios of 1:1, 2:1, and 3:1 for P1, P2, and P3 samples, respectively. Each series of samples consist of two samples, with those with suffix 1 representing low-block number (i.e., molecular weight) samples while 2 for high-block number mBCPs. The block number was controlled by adjusting the PROP polymerization time and temperature.

The architecture of mBCPs was characterized by ¹H quantitative NMR experiments (Figure S1 and Table S2). The weight ratio of PBT to PTMO was calculated from the integration value of phenyl groups (peak p) of PBT to methylene oxide groups (peak i) of PTMO. The estimated weight content of PTMO in mBCPs is around 50, 67, and 77% for P1, P2, and P3 samples, similar to their feeding weight content, indicating the good control of mBCPs' architecture by PROP. In addition, with the distinguishing of methylene hydroxide (CH2OH) chain-end groups (peak a), the total number of PBT and PTMO repeat units in (PBT-b-PTMO-b-PBT), mBCPs can be calculated, together with the whole number-average molecular weight (M_n) and the repeat unit number (n) of PBT-b-PTMO-b-PBT segments.⁴⁸ The total block number (N) is estimated as 2n + 1. The results are summarized in Table 1.

The viscosity of the six $(PBT-b-PTMO-b-PBT)_n$ samples was measured to test the reliability of NMR techniques. The intrinsic viscosity was deduced by the extrapolation of measured viscosities at different concentrations in phenol/1,1,2,2-tetrachloroethane (6/4 in mass ratio) solvent to the infinite dilution condition. ⁵³ The obtained results are provided

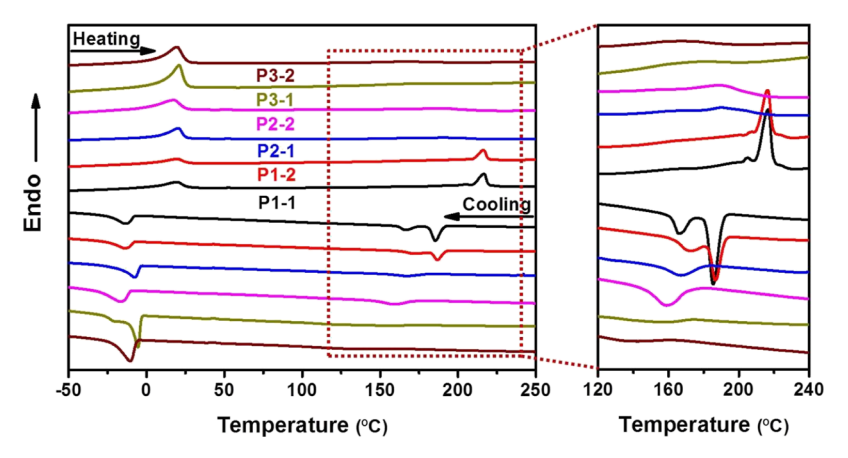


Figure 2. Second heating and first cooling DSC curves of $(PBT-b-PTMO-b-PBT)_n$ mBCPs, with the corresponding region related to PBT blocks enlarged on the right side. Condition: N_{2j} scanning rate: 10 °C min⁻¹.

Table 2. Thermal Properties and Phase-Separation Size of (PBT-b-PTMO-b-PBT), mBCPs

		P	TMO				PBT			
sample	$T_{\rm m}^{a}$ (°C)	T_c^b (°C)	$\Delta H_{\rm m}^{c} (J/g)$	ΔH_c^c (J/g)	$T_{\rm m}^{a}$ (°C)	T_c^b (°C)	$\Delta H_{\rm m}^{c} (J/g)$	ΔH_c^c (J/g)	$X_{\rm c}^{d}$ (%)	d^e (nm)
P1-1	19.9	-13.9	13.3	12.9	216.8	185.6	17.1	16.4	23.5	30
P1-2	19.9	-13.9	10.8	10.3	216.2	186.6	13.4	11.2	18.4	22
P2-1	20.5	-7.6	19.1	18.3	190.2	166.9	9.8	6.2	20.2	35
P2-2	17.8	-10.5	16.7	16.1	190.1	145.6	6.8	5.7	14.0	33
P3-1	20.9	-5.5	36.4	35.2	179.8	154.6	2.9	2.4	8.0	
P3-2	19.7	-10.5	28.8	24.2	167.1	139.5	2.5	2.3	6.9	37

[&]quot;Melting temperature of the corresponding blocks. "Crystallization temperature of the corresponding blocks. "Normalized melting/crystallization enthalpy calculated by the corresponding values measured by DSC divided by the weight fraction of the corresponding blocks. "Degree of crystallinity calculated from the enthalpy of the second heating curve by $X_c = \Delta H_{\rm m}/\Delta H_{\rm m}^0$, where $\Delta H_{\rm m}^0$ is the enthalpy value of melting of the 100% crystalline form of PBT (145.5 J/g). "Phase-separation size measured by SAXS.

in Table 1, which coincide well with that from ¹H NMR spectra as those mBCPs with bigger intrinsic viscosity show higher molecular weights.

All (PBT-b-PTMO-b-PBT), samples have good thermal stability, with 5% weight loss temperature at around 350 °C, from thermogravimetric analysis (Figure S2). The mBCPs with different PBT contents have similar thermal weight loss temperatures, indicating that the thermal stability of the copolymer is not affected by the change in PBT content. The second heating and first cooling differential scanning calorimetry (DSC) curves for those samples are presented in Figure 2, with the corresponding region related to PBT blocks enlarged at the right side, and the results are summarized in Table 2. For all six $(PBT-b-PTMO-b-PBT)_n$ samples, they are double-crystalline polymers as two separated melting peaks $(T_{\rm m})$ during heating and two crystallization peaks $(T_{\rm c})$ during cooling are observed. The high-temperature peaks are assigned to PBT blocks, while the low-temperature peaks are assigned to PTMOs. The peak transition temperatures $(T_{\rm m}$ and $T_{\rm c})$ corresponding to PBT blocks increase with PBT content in mBCPs, indicating the formation of more perfect (thicker) crystals. This is supported by the increment of PBT's normalized melting enthalpy (ΔH_m) (Table 2). It is reasonable since the PBT's segment length (S_{BT}) increases with PBT content as the PTMO's segment length is fixed during

For PTMO blocks, their peak transition temperatures ($T_{\rm m}$ and $T_{\rm c}$) decrease slightly with the increment of PBT content, but their normalized melting/crystallization enthalpies decrease significantly. This indicates that less PTMO segments

are crystallized while their segment length is the same in all samples. Considering that PBTs form lamellar crystals first during cooling, PTMO segments have to be crystallized on the surface of PBT crystals due to the covalent connection between them. Increasing PBT content means more PBT crystal surface to be covered, thus the crystal thickness of PTMOs is reduced. In addition, according to Flory's switchboard model, PBT segments from the same mBCP chain can shuttle between different lamellar crystals. The shuttling chance increases with the PBT content, and the middle PTMO chain among two shuttling chains is so strained that it cannot be crystallized.

The effect of block number on the thermal behavior of mBCPs is interesting. For P1 samples, both the peak transition temperatures for PTMO and PBT blocks are not affected by the block numbers. However, the crystallinity for both PTMO and PBT blocks in P1-1 is larger than that in P1-2 mBCPs, indicating the decrement of crystallinity with the increment of block number. For P2 and P3 samples, the melting and crystallization peak transition temperatures and crystallinity for PTMO and PBT blocks decrease slightly with the increment of block numbers too. This is due to the reduced phase-separation-domain size, which will be discussed in the following part.

At temperatures higher than PBT's melting temperature, PBT and PTMO should be miscible since no peak in the small-angle X-ray scattering (SAXS) region was detected (Figure S3). This is consistent with previous reports about poly(ether ester) mBCPs. ^{56–58} During cooling, phase separation occurred due to PBT crystallization. After cooling to room temperature

(~25 °C), PTMO blocks should be in the amorphous state since it is slightly higher than their melting point. This is supported by the wide-angle X-ray scattering results, where only peaks related to PBT crystals were observed (Figure S4).

SAXS experiments were carried out to investigate the phase separation of mBCPs at room temperature, with the curves being presented in Figure 3. For the P1-1 sample, the two

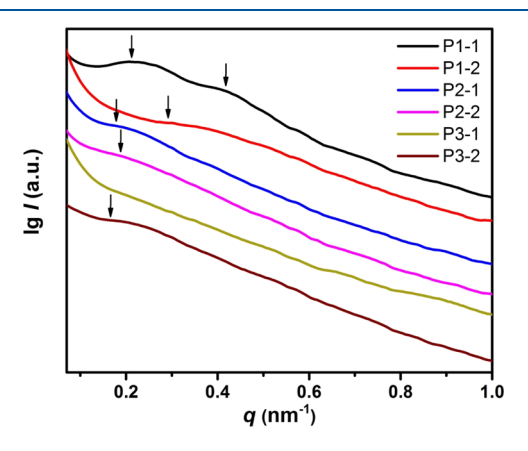


Figure 3. SAXS profiles of (PBT-*b*-PTMO-*b*-PBT)_n mBCPs. The arrow indicates the peak position for the corresponding SAXS curves.

peaks (0.21 and 0.42 nm⁻¹) observed indicate a lamellar structure. For P1-2, P2-1, P2-2, and P3-2 samples, there is only one relatively broad peak observed at 0.29, 0.18, 0.19, and 0.17 nm⁻¹, respectively, indicating that the structure of domains is not well-ordered. Meanwhile, no obvious peak was observed in P3-1, suggesting a more poorly ordered structure. Their corresponding phase-separation-domain size (*d*) is provided in Table 2. For P1 and P2 samples, the size decreases with the increment of block number. This can be assigned to the increased bulk viscosity that limits the diffusion of chain segments and hinders the well development of phase-separation domains.

The less-ordered phase-separation structures observed here are quite different to those of recently reported BCPs, where distinct peaks are observed from those monodispersed samples by SAXS. $^{59-64}$ However, in the elegant works reported by Bates' group about polyolefin-based crystalline mBCPs, the ordered lamellar structure changed to a disordered bicontinuous morphology at a high block number ($n \ge 9$). Since the block numbers in our system are high (>7) except P1-1, our results suggest the formation of a similar disordered bicontinuous morphology.

For copolymers with a similar block number, P1-2 has a much smaller domain size than P2-1 samples. It suggests that the increment of polyester content reduces the phase-separation-domain size. This can be explained by the reduced lamellar thickness of PTMOs with the increment of PBT content to cover more PBT crystal surface area, thus the phase-separation-domain size is decreased as shown in Figure 4a. The results coincide well with that from DSC experiments.

To further investigate the phase-separation morphologies, (PBT-b-PTMO-b-PBT)_n mBCPs were microtomed and stained with 0.2 wt % phosphotungstic acid (PTA), and their transmission electron microscopy (TEM) images are shown in Figure 5. As PTA prefers to stain amorphous PTMO domains, the dark-colored regions are assigned to the PTMO-rich region while the light-colored regions to PBT-rich domains. The

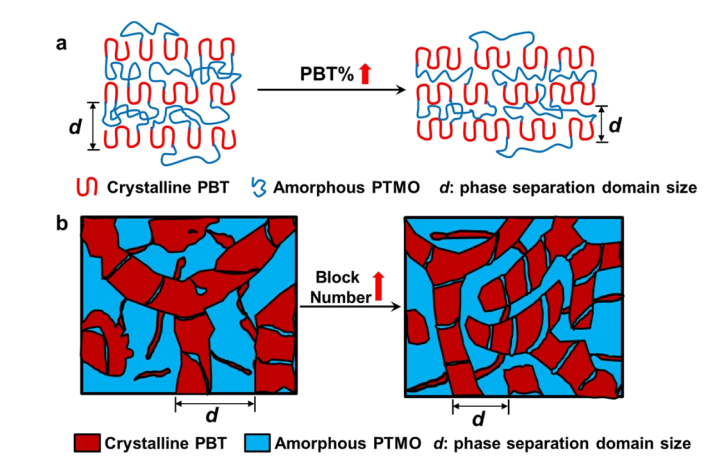


Figure 4. Schematic illustration of microphase separation of (PBT-b-PTMO-b-PBT) $_n$ mBCPs with increased polyester contents (a) and block numbers (b).

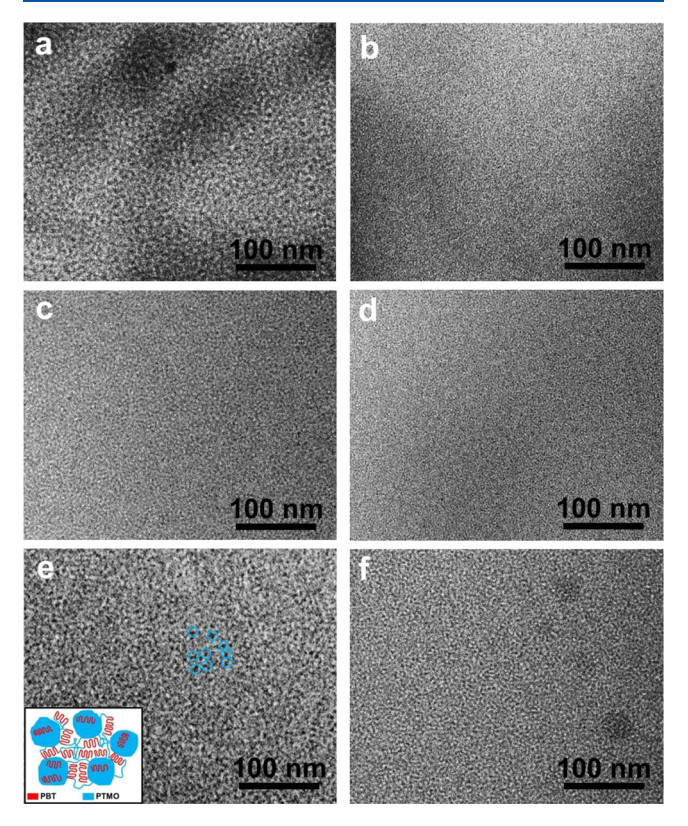


Figure 5. TEM images of $(PBT-b-PTMO-b-PBT)_n$ mBCPs: P1-1 (a), P1-2 (b), P2-1 (c), P2-2 (d), P3-1 (e), and P3-2 (f). The blue circles in (e) represent the PTMO-rich microemulsion-like domains, while the inset shows a plausible bicontinuous phase model with interpenetrating PBT and PTMO blocks.

mBCPs show a similar hierarchical interpenetrating bicontinuous phase, despite their volume fraction. Among the PTMOrich and PBT-rich region, a small-length scale light-colored or dark-colored lamellar-like structure can be observed when enlarged. The hierarchical structure is somewhat similar to the double-periodic lamellar-in-lamellar structure reported in mBCPs. and close to that observed by Bates' group in crystalline mBCPs, where they ascribed it as a bicontinuous microemulsion-like disordered phase.

The phase-separation size observed by TEM is smaller than that from SAXS, as more sophisticated fine structures can be revealed by TEM even if they are less ordered. In these samples, the PBT crystalline lamellae have the thickness of approximately 3–10 nm. Since the lamella thickness observed from TEM is much smaller than that observed from SAXS, the associate correlation hole scattering in SAXS may come from the distance between PTMO-rich microemulsion domains, as shown in the inset of Figure 5e.

With the increment of block numbers, in all three series of samples, the phase—separation-domain size and the PBT lamellar thickness decrease. The result is in good agreement with that obtained from SAXS and supports our assumptions in the explanation for the melting and crystallization behaviors of mBCPs. The schematic illustration is presented in Figure 4b.

Since typical poly(ether ester) copolymers are elastomers with good resilience, 70,71 the mechanical properties of all six (PBT-*b*-PTMO-*b*-PBT)_n mBCPs were measured to reveal the structure—property relationship. The stress—strain curves are presented in Figure 6. All copolymers have a relatively typical

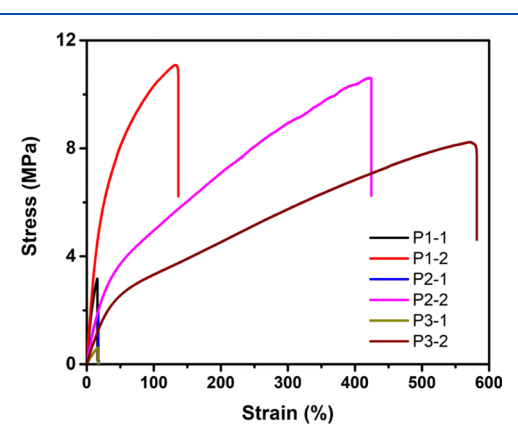


Figure 6. Stress-strain curves of (PBT-b-PTMO-b-PBT), mBCPs.

elastic Young's modulus, among 4–34 MPa. As PBTs are the load-bearing domains in mBCPs, the Young's modulus increases with their content. The mechanical properties are summarized in Table 3.

Table 3. Tensile Properties of $(PBT-b-PTMO-b-PBT)_n$ mBCPs

sample	Young's modulus (MPa)	tensile strength (MPa)	elongation at break (%)
P1-1	25 ± 1.2	3.2 ± 1.1	16 ± 1
P1-2	34 ± 1.8	11.1 ± 0.5	134 ± 15
P2-1	13.1 ± 0.6	1.9 ± 0.2	17 ± 2
P2-2	12.5 ± 0.5	10.6 ± 0.5	423 ± 31
P3-1	4.2 ± 0.2	0.62 ± 0.1	16 ± 2
P3-2	7.9 ± 0.2	8.2 ± 0.3	575 ± 42

For copolymers with a similar composition, their tensile strength and elongation at break increase significantly with the increment of block number. This can be explained by the enhanced portion of bridging and entangled looping segments between different domains, which resists the chains pulling out from crystal domains. ^{9,30,72} On the other hand, the Young's modulus is less affected by the block number, since PBT content is not changed.

CONCLUSIONS

The effects of polyester weight fraction and total block number on the properties of a series of (PBT-b-PTMO-b-PBT)... mBCPs are studied. Our results show that the crystallization temperature, melting temperature, and crystallinity of the PBT blocks increase with the PBT content, while those of PTMOs are less affected. The crystallinity decreased with increasing block numbers due to the formation of smaller phaseseparation domains. These mBCPs form a hierarchical bicontinuous disordered phase-separation morphology with PBT lamellar crystals embedded in them. Their Young's modulus increases with the PBT content, while the stress and strain at break increase significantly with block number due to the enhanced segments with bridging and looping configurations between different domains. Our results reveal the effect of block number on the crystallinity, phase-separation structure, and mechanical properties of mBCPs and provide a strategy to tune the mechanical properties of mBCPs by changing their architecture.

ASSOCIATED CONTENT

Supporting Information

The Supporting Information is available free of charge at https://pubs.acs.org/doi/10.1021/acs.macromol.0c02793.

Experimental conditions for polymer synthesis and characterization; ¹H quantitative NMR results of COBTs, PTMO, and mBCPs; X-ray diffraction profiles of mBCPs; thermogravimetric analysis curves of mBCPs and PTMO2.9 k; and WAXD curves of mBCPs, PTMO2.9 k, and PBT (PDF)

AUTHOR INFORMATION

Corresponding Author

Yingfeng Tu — Jiangsu Key Laboratory of Advanced Functional Polymer Design and Application, College of Chemistry, Chemical Engineering and Materials Science, Soochow University, Suzhou 215123, China; orcid.org/0000-0001-6221-9145; Email: tuyingfeng@suda.edu.cn

Authors

Hui Xie – Jiangsu Key Laboratory of Advanced Functional Polymer Design and Application, College of Chemistry, Chemical Engineering and Materials Science, Soochow University, Suzhou 215123, China

Huanjun Lu – Jiangsu Key Laboratory of Advanced Functional Polymer Design and Application, College of Chemistry, Chemical Engineering and Materials Science, Soochow University, Suzhou 215123, China

Zhilan Zhang — Jiangsu Key Laboratory of Advanced Functional Polymer Design and Application, College of Chemistry, Chemical Engineering and Materials Science, Soochow University, Suzhou 215123, China

Xiaohong Li − Jiangsu Key Laboratory of Advanced Functional Polymer Design and Application, College of Chemistry, Chemical Engineering and Materials Science, Soochow University, Suzhou 215123, China; orcid.org/0000-0003-3190-7214

Xiaoming Yang — Jiangsu Key Laboratory of Advanced Functional Polymer Design and Application, College of Chemistry, Chemical Engineering and Materials Science, Soochow University, Suzhou 215123, China; Orcid.org/0000-0002-5324-7416

Complete contact information is available at: https://pubs.acs.org/10.1021/acs.macromol.0c02793

Author Contributions

[†]H.X. and H.L. contributed equally to this work.

Notes

The authors declare no competing financial interest.

ACKNOWLEDGMENTS

Financial support from the National Key R&D Program of China (2018YFB1105700), the National Natural Science Foundation of China (grant nos 22071167 and 21774090), and a project funded by the Priority Academic Program Development of Jiangsu Higher Education Institutions is gratefully acknowledged.

REFERENCES

- (1) Russell, T. P.; Karis, T. E.; Gallot, Y.; Mayes, A. M. A Lower Critical Ordering Transition in a Diblock Copolymer Melt. *Nature* **1994**, *368*, 729–731.
- (2) Hamley, I. The Physics of Block Copolymers; Oxford University Press, 1998; p 432.
- (3) Adhikari, R.; Michler, G. H. Influence of Molecular Architecture on Morphology and Micromechanical Behavior of Styrene/Butadiene Block copolymer Systems. *Polym. Sci.* **2004**, *29*, 949–986.
- (4) Sing, C. E.; Zwanikken, J. W.; Olvera de la Cruz, M. Elestrostatic Control of Block Copolymer Morphology. *Nat. Mater.* **2014**, *13*, 694–698.
- (5) Gao, L.; Ji, Z.; Zhao, Y.; Cai, Y.; Li, X.; Tu, Y. Synthesis and Solution Self-Assembly Properties of Cyclic Rod-Coil Diblock Copolymers. ACS Macro Lett. 2019, 8, 1564–1569.
- (6) Lynd, N. A.; Meuler, A. J.; Hillmyer, M. A. Polydispersity and Block Copolymer Self-Assembly. *Prog. Polym. Sci.* **2008**, *33*, 875–893.
- (7) Roy, R.; Park, J. K.; Young, W.-S.; Mastroianni, S. E.; Tureau, M. S.; Epps, T. H. Double-Gyroid Network Morphology in Tapered Diblock Copolymers. *Macromolecules* **2011**, *44*, 3910–3915.
- (8) Mu, D.; Li, J.-Q.; Feng, S.-Y. Morphology of Lipid-Like Structured Weak Polyelectrolyte Poly(ethylene oxide)-block-Poly(methyl methacrylate) Diblock Copolymers Induced by Confinements. *Soft Matter* **2015**, *11*, 4356–4365.
- (9) Lee, I.; Panthani, T. R.; Bates, F. S. Sustainable Poly(lactide-b-butadiene) Multiblock Copolymers with Enhanced Mechanical Properties. *Macromolecules* **2013**, *46*, 7387–7398.
- (10) Zhang, M.; Gu, J.; Zhu, X.; Gao, L.; Li, X.; Yang, X.; Tu, Y.; Li, C. Y. Synthesis of Poly(butylene terephthalate)-block-Poly(ethylene oxide)-block-Poly(propylene oxide)-block-Poly(ethylene oxide) Multiblock Terpolymers via a Facile PROP Method. *Polymer* 2017, 130, 100–208
- (11) Zhang, J.; Deubler, R.; Hartlieb, M.; Martin, L.; Tanaka, J.; Patyukova, E.; Topham, P. D.; Schacher, F. H.; Perrier, S. Evolution of Microphase Separation with Variations of Segments of Sequence-Controlled Multiblock Copolymers. *Macromolecules* **2017**, *50*, 7380–7387.
- (12) Steube, M.; Johann, T.; Galanos, E.; Appold, M.; Rüttiger, C.; Mezger, M.; Gallei, M.; Müller, A. H. E.; Floudas, G.; Frey, H. Isoprene/Styrene Tapered Multiblock Copolymers with up to Ten Blocks: Synthesis, Phase Behavior, Order, and Mechanical Properties. *Macromolecules* **2018**, *51*, 10246–10258.
- (13) Xie, Q.; Qiang, Y.; Zhang, G.; Li, W. Emergence and Stability of Janus-Like Superstructures in an ABCA Linear Tetrablock Copolymer. *Macromolecules* **2020**, *53*, 7380–7388.
- (14) Zheng, Y.; Weng, C.; Cheng, C.; Zhao, J.; Yang, R.; Zhang, Q.; Ding, M.; Tan, H.; Fu, Q. Multiblock Copolymers toward Segmentation-Driven Morphological Transition. *Macromolecules* **2020**, *53*, 5992–6001.

- (15) Bates, F. S.; Hillmyer, M. A.; Lodge, T. P.; Bates, C. M.; Delaney, K. T.; Fredrickson, G. H. Multiblock Polymers: Panacea or Pandora's Box? *Science* **2012**, *336*, 434–440.
- (16) Coca, S.; Matyjaszewski, K. Block Copolymers by Transformation of "Living" Carbocationic into "Living" Radical Polymerization. *Macromolecules* **1997**, *30*, 2808–2810.
- (17) Kwon, Y.; Cao, X.; Faust, R. Synthesis of Poly(α -methylstyreneb-isobutylene) Copolymers by Living Cationic Sequential Block Copolymerization: Investigation on The Crossover From Living Poly(α -methylstyrene) Chain End to Isobutylene. *Macromolecules* 1999, 32, 6963–6968.
- (18) Wang, W.; Li, T.; Yu, T.; Zhu, F. Synthesis of Multiblock Copolymers by Coupling Reaction Based on Self-Assembly and Click Chemistry. *Macromolecules* **2008**, *41*, 9750–9754.
- (19) Su, M.; Liu, N.; Wang, Q.; Wang, H.; Yin, J.; Wu, Z.-Q. Facile Synthesis of Poly(phenyleneethynylene)-block-Polyisocyanide Copolymers via Two Mechanistically Distinct, Sequential Living Polymerizations Using a Single Catalyst. *Macromolecules* **2016**, 49, 110–119.
- (20) Yang, L.; Ma, H.; Han, L.; Liu, P.; Shen, H.; Li, C.; Li, Y. Sequence Features of Sequence-Controlled Polymers Synthesized by 1,1-Diphenylethylene Derivatives with Similar Reactivity during Living Anionic Polymerization. *Macromolecules* **2018**, *51*, 5891–5903.
- (21) Yang, L.; Shen, H.; Han, L.; Ma, H.; Li, C.; Lei, L.; Zhang, S.; Liu, P.; Li, Y. Sequence regulation in living anionic terpolymerization of styrene and two categories of 1,1-diphenylethylene (DPE) derivatives. *Polym. Chem.* **2020**, *11*, 5163–5172.
- (22) Kanazawa, A.; Aoshima, S. Cationic Copolymerization of Styrene Derivatives and Oxiranes via Concurrent Vinyl-Addition and Ring-Opening Mechanisms: Multiblock Copolymer Formation via Occasional Crossover Reactions. *Macromolecules* **2020**, *53*, 5255–5265.
- (23) Lamparelli, D. H.; Paradiso, V.; Monica, F. D.; Proto, A.; Guerra, S.; Giannini, L.; Capacchione, C. Toward More Sustainable Elastomers: Stereoselective Copolymerization of Linear Terpenes with Butadiene. *Macromolecules* **2020**, *53*, 1665–1673.
- (24) Adhikari, R.; Michler, G. H. Influence of Molecular Architecture on Morphology and Micromechanical Behavior of Styrene/Butadiene Block Copolymer Systems. *Prog. Polym. Sci.* **2004**, *29*, 949–986.
- (25) Nagata, Y.; Masuda, J.; Noro, A.; Cho, D.; Takano, A.; Matsushita, Y. Preparation and Characterization of a Styrene-Isoprene Undecablock Copolymer and its Hierarchical Microdomain Structure in Bulk. *Macromolecules* **2005**, *38*, 10220–10225.
- (26) Gibson, V. C. Shuttling Polyolefins to a New Materials Dimension. *Science* **2006**, *312*, 703–704.
- (27) Flores, I.; Basterretxea, A.; Etxeberria, A.; González, A.; Ocando, C.; Vega, J. F.; Martínez-Salazar, J.; Sardon, H.; Müller, A. J. Organocatalyzed Polymerization of PET-mb-poly(oxyhexane) Copolymers and Their Self-Assembly into Double Crystalline Superstructures. *Macromolecules* **2019**, *52*, 6834–6848.
- (28) Fang, J.; Gao, X.; Luo, Y. Synthesis of (hard-soft-hard)(x) Multiblock Copolymers via RAFT Emulsion Polymerization and Mechanical Enhancement via Block Architectures. *Polymer* **2020**, 201, 122602
- (29) Bates, F. S.; Fredrickson, G. H.; Hucul, D.; Hahn, S. F. PCHE-Based Pentablock Copolymers: Evolution of a New Plastic. *AIChE J.* **2001**, *47*, 762–765.
- (30) Hermel, T. J.; Hahn, S. F.; Chaffin, K. A.; Gerberich, W. W.; Bates, F. S. Role of Molecular Architecture in Mechanical Failure of Glassy/Semicrystalline Block Copolymers: CEC vs CECEC Lamellae. *Macromolecules* **2003**, *36*, 2190–2193.
- (31) Xu, J.; Eagan, J. M.; Kim, S.-S.; Pan, S.; Lee, B.; Klimovica, K.; Jin, K.; Lin, T.-W.; Howard, M. J.; Ellison, C. J.; LaPointe, A. M.; Coates, G. W.; Bates, F. S. Compatibilization of Isotactic Polypropylene (iPP) and High-Density Polyethylene (HDPE) with iPP-PE Multiblock Copolymers. *Macromolecules* **2018**, *51*, 8585–8596.

- (32) Vigild, M. E.; Chu, C.; Sugiyama, M.; Chaffin, K. A.; Bates, F. S. Influence of Shear on The Alignment of a Lamellae-Forming Pentablock Copolymer. *Macromolecules* **2001**, *34*, 951–964.
- (33) Fleury, G.; Bates, F. S. Structure and Properties of Hexa- and Undecablock Terpolymers with Hierarchical Molecular Architectures. *Macromolecules* **2009**, *42*, 3598–3610.
- (34) Bates, C. M.; Bates, F. S. 50th Anniversary Perspective: Block Polymers-Pure Potential. *Macromolecules* **2017**, *50*, 3–22.
- (35) Hermel, T. J.; Wu, L.; Hahn, S. F.; Lodge, T. P.; Bates, F. S. Shear-Induced Lamellae Alignment in Matched Triblock and Pentablock Copolymers. *Macromolecules* **2002**, *35*, 4685–4689.
- (36) Szymczyk, A.; Senderek, E.; Nastalczyk, J.; Roslaniec, Z. New Multiblock Poly(ether ester)s Based on Poly(trimethylene terephthalate) as Rigid Segments. *Eur. Polym. J.* **2008**, *44*, 436–443.
- (37) Lee, I.; Bates, F. S. Synthesis, Structure, and Properties of Alternating and Random Poly(styrene-b-butadiene) Multiblock Copolymers. *Macromolecules* **2013**, *46*, 4529–4539.
- (38) Steube, M.; Johann, T.; Galanos, E.; Appold, M.; Rüttiger, C.; Mezger, M.; Gallei, M.; Müller, A. H. E.; Floudas, G.; Frey, H. Isoprene/Styrene Tapered Multiblock Copolymers with up to Ten Blocks: Synthesis, Phase Behavior, Order, and Mechanical Properties. *Macromolecules* **2018**, *51*, 10246–10258.
- (39) Steube, M.; Johann, T.; Hübner, H.; Koch, M.; Dinh, T.; Gallei, M.; Floudas, G.; Frey, H.; Müller, A. H. E. Tetrahydrofuran: More than a "Randomizer" in the Living Anionic Copolymerization of Styrene and Isoprene: Kinetics, Microstructures, Morphologies, and Mechanical Properties. *Macromolecules* **2020**, *53*, 5512–5527.
- (40) Szwarc, M.; Levy, M.; Milkovich, R. Polymerization Initiated by Electron Transfer to Monomer. A New Method of Formation of Block Polymers. *J. Am. Chem. Soc.* **1956**, *78*, 2656–2657.
- (41) Kwon, Y.; Cao, X.; Faust, R. Synthesis of Poly(α -methylstyreneb-isobutylene) Copolymers by Living Cationic Sequential Block Copolymerization: Investigation on The Crossover From Living Poly(α -methylstyrene) Chain End to Isobutylene. *Macromolecules* **1999**, 32, 6963–6968.
- (42) Wang, W.; Li, T.; Yu, T.; Zhu, F. Synthesis of Multiblock Copolymers by Coupling Reaction Based on Self-Assembly and Click Chemistry. *Macromolecules* **2008**, *41*, 9750–9754.
- (43) Mizutani, M.; Satoh, K.; Kamigaito, M. Metal-Catalyzed Radical Polyaddition for Aliphatic Polyesters via Evolution of Atom Transfer Radical Addition into Step-Growth Polymerization. *Macromolecules* **2009**, *42*, 472–480.
- (44) Xia, Y.; Chen, Y.; Song, Q.; Hu, S.; Zhao, J.; Zhang, G. Base-to-Base Organocatalytic Approach for One-Pot Construction of Poly(ethylene oxide)-Based Macromolecular Structures. *Macromolecules* **2016**, 49, 6817–6825.
- (45) Easterling, C. P.; Xia, Y.; Zhao, J.; Fanucci, G. E.; Sumerlin, B. S. Block Copolymer Sequence Inversion through Photoiniferter Polymerization. *ACS Macro Lett.* **2019**, *8*, 1461–1466.
- (46) Kwak, S.-Y.; Nakajima, N. Morphology Formation in Mixing of Copolyester Thermoplastic Elastomer (Hytrel) with Poly(vinyl chloride) and Nuclear Magnetic Resonance Relaxation Study on Solid Structures of the Mixture. *Macromolecules* 1996, 29, 3521–3524.
- (47) Xu, Q.; Chen, J.; Huang, W.; Qu, T.; Li, X.; Li, Y.; Yang, X.; Tu, Y. One pot, One Feeding Step, Two-stage Polymerization Synthesis and Characterization of (PTT-b-PTMO-b-PTT)_n Multiblock Copolymers. *Macromolecules* **2013**, *46*, 7274–7281.
- (48) Chen, J.; Chen, D.; Huang, W.; Yang, X.; Li, X.; Tu, Y.; Zhu, X. A One Pot Facile Synthesis of Poly(butylene terephthalate)-block-Poly(tetramethylene oxide) Alternative Multiblock Copolymers via PROP Method. *Polymer* **2016**, *107*, 29–36.
- (49) Tu, Y.-f. Cascade Polymerization. *Acta Polym. Sin.* **2019**, *50*, 1146–1155.
- (50) Xu, S.; Wu, F.; Li, Z.; Zhu, X.; Li, X.; Wang, L.; Li, Y.; Tu, Y. A Green Cascade Polymerization Method for the Facile Synthesis of Sustainable Poly(butylene-co-decylene terephthalate) Copolymers. *Polymer* **2019**, *178*, 121591.
- (51) Wang, W.; Wu, F.; Lu, H.; Li, X.; Yang, X.; Tu, Y. A Cascade Polymerization Method for the Property Modification of Poly-

- (butylene terephthalate) by the Incorporation of Isosorbide. ACS Appl. Polym. Mater. 2019, 1, 2313–2321.
- (\$2) Li, Z.; Wang, J.; Li, X.; Wang, Y.; Fan, L.-J.; Yang, S.; Guo, M.; Li, X.; Tu, Y. Supramolecular and Physically Double-Cross-Linked Network Strategy toward Strong and Tough Elastic Fibers. ACS Macro Lett. 2020, 9, 1655–1661.
- (53) Li, K.; Song, X.; Zhang, D. Molecular Weight Evaluation of Depolymerized Poly(ethylene terephthalate) Using Intrinsic Viscosity. *J. Appl. Polym. Sci.* **2008**, *109*, 1294–1297.
- (54) Flory, P. J. On Morphology of Crystalline State in Polymers. J. Am. Chem. Soc. 1962, 84, 2857.
- (55) Chen, J.; Huang, W.; Xu, Q.; Tu, Y.; Zhu, X.; Chen, E. PBT-b-PEO-b-PBT Triblock Copolymers: Synthesis, Characterization and Double-Crystalline Properties. *Polymer* **2013**, *54*, 6725–6731.
- (56) Gabriëlse, W.; Soliman, M.; Dijkstra, K. Microstructure and Phase Behavior of Block Copoly(ether ester) Thermoplastic Elastomers. *Macromolecules* **2001**, *34*, 1685–1693.
- (57) Litvinov, V. M.; Bertmer, M.; Gasper, L.; Demco, D. E.; Blümich, B. Phase Composition of Block Copoly(ether ester) Thermoplastic Elastomers Studied by Solid-State NMR Techniques. *Macromolecules* **2003**, *36*, 7598–7606.
- (58) Nébouy, M.; de Almeida, A.; Brottet, S.; Baeza, G. P. Process-Oriented Structure Tuning of PBT/PTHF Thermoplastic Elastomers. *Macromolecules* **2018**, *51*, 6291–6302.
- (59) Rosenbloom, S. I.; Fors, B. P. Shifting Boundaries: Controlling Molecular Weight Distribution Shape for Mechanically Enhanced Thermoplastic Elastomers. *Macromolecules* **2020**, *53*, 7479–7486.
- (60) Gao, J.; Lv, C.; An, K.; Gu, X.; Nie, J.; Li, Y.; Xu, J.; Du, B. Observation of Double Gyroid and Hexagonally Perforated Lamellar Phases in ABCBA Pentablock Terpolymers. *Macromolecules* **2020**, *53*, 9641–9653.
- (61) Wahlen, C.; Blankenburg, J.; von Tiedemann, P.; Ewald, J.; Sajkiewicz, P.; Müller, A. H. E.; Floudas, G.; Frey, H. Tapered Multiblock Copolymers Based on Farnesene and Styrene: Impact of Biobased Polydiene Architectures on Material Properties. *Macromolecules* **2020**, *53*, 10397–10408.
- (62) Bates, M. W.; Barbon, S. M.; Levi, A. E.; Lewis, R. M.; Beech, H. K.; Vonk, K. M.; Zhang, C.; Fredrickson, G. H.; Hawker, C. J.; Bates, C. M. Synthesis and Self-Assembly of AB_n Miktoarm Star Polymers. *ACS Macro Lett.* **2020**, *9*, 396–403.
- (63) Yang, K.-C.; Ho, R.-M. Spiral Hierarchical Superstructures from Twisted Ribbons of Self-Assembled Chiral Block Copolymers. *ACS Macro Lett.* **2020**, *9*, 1130–1134.
- (64) Barbon, S. M.; Song, J.-A.; Chen, D.; Zhang, C.; Lequieu, J.; Delaney, K. T.; Anastasaki, A.; Rolland, M.; Fredrickson, G. H.; Bates, M. W.; Hawker, C. J.; Bates, C. M. Architecture Effects in Complex Spherical Assemblies of (AB)_n-Type Block Copolymers. *ACS Macro Lett.* **2020**, *9*, 1745–1752.
- (65) Koo, C. M.; Hillmyer, M. A.; Bates, F. S. Structure and Properties of Semicrystalline-Rubbery Multiblock Copolymers. *Macromolecules* **2006**, *39*, 667–677.
- (66) Zuo, F.; Alfonzo, C. G.; Bates, F. S. Structure and Mechanical Behavior of Elastomeric Multiblock Terpolymers Containing Glassy, Rubbery, and Semicrystalline Blocks. *Macromolecules* **2011**, *44*, 8143–8153
- (67) Nap, R.; Sushko, N.; Erukhimovich, I.; ten Brinke, G. Double Periodic Lamellar-in-Lamellar Structure in Multiblock Copolymer Melts with Competing Length Scales. *Macromolecules* **2006**, 39, 6765–6770.
- (68) Subbotin, A.; Markov, V.; ten Brinke, G. Parallel versus Perpendicular Lamellar-within-Lamellar Self-Assembly of A-b-(B-b-A)_n-b-C Ternary Multiblock Copolymer Melts. *J. Phys. Chem. B* **2010**, 114, 5250–5256.
- (69) Hong, W.; Lin, J.; Tian, X.; Wang, L. Distinct Viscoelasticity of Hierarchical Nanostructures Self-Assembled from Multiblock Copolymers. *Macromolecules* **2020**, *53*, 10955–10963.
- (70) Schmalz, H.; Abetz, V.; Lange, R.; Soliman, M. New Thermoplastic Elastomers by Incorporation of Nonpolar Soft

Segments in PBT-Based Copolyesters. *Macromolecules* **2001**, *34*, 795–800.

- (71) Xie, H.; Wu, L.; Li, B.-G.; Dubois, P. Poly(ethylene 2,5-furandicarboxylate-mb-Poly(tetramethylene glycol)) Multiblock Copolymers: From High Tough Thermoplastics to Elastomers. *Polymer* **2018**, *155*, 89–98.
- (72) Eagan, J. M.; Xu, J.; Di Girolamo, R.; Thurber, C. M.; Macosko, C. W.; LaPointe, A. M.; Bates, F. S.; Coates, G. W. Combining Polyethylene and Polypropylene: Enhanced Performance with PE/iPP Multiblock Polymers. *Science* **2017**, 355, 814–816.